Layered titanate–zinc oxide nanohybrids with mesoporosity†

Tae Woo Kim, Su Gil Hur, Seong-Ju Hwang* and Jin-Ho Choy*

Received (in Cambridge, UK) 11th August 2005, Accepted 19th October 2005
First published as an Advance Article on the web 21st November 2005
DOI: 10.1039/b511471c

Zinc oxide-layered titanate nanohybrids with a 1 : 1 ordered heterostructure have been successfully synthesized by reassembling exfoliated titanate nanosheets in the sol solution of zinc acetate under hydrothermal conditions.

Recently nanostructured zinc oxide has attracted intense research interest since it has wide applications as luminescent and lasing materials, light emitting diodes, photocatalysts, solar cells, and so on.[1–4] Such useful functionalities of this material originate mainly from its wide bandgap and its specific electrical and optoelectronic properties of being a II–VI semiconductor with a large exciton energy.[5] In this regard, many research activities have been devoted to this material, leading to the development of various synthetic routes to nanostructured ZnO such as hydrothermal synthesis, the vapour-transport reaction, reverse micelles synthesis, *etc*.[6–8] A crystal growth of ZnO in the limited interlayer space of 2D inorganic solids is expected to provide an alternative and effective way of synthesizing nanocrystalline zinc oxides. Moreover, the hybridization of ZnO with layered metal oxide semiconductors makes it possible to tailor electronic structure and physical properties of the guest zinc oxide through the electronic coupling between both components. Also, the resulting mesoporous ZnO-based nanohybrid would possess enhanced catalytic and electrochemical activity due to the expansion of surface area. However, despite intense research activities on 0D nanoparticles and 1D nanorods/nanowires of ZnO,[1,6–8] a 2D heterostructure of zinc oxide-layered metal oxide has never been synthesized, which will be due to the poor swelling ability of the host layered metal oxide. In order to circumvent this difficulty, we have adopted an exfoliation-restacking method, in which the layered lattice of metal oxide is separated into individual monosheets and then hybridized with guest species.[9] In this work, we have synthesized, for the first time, mesoporous nanohybrids interstratified with zinc oxide nanoparticles and layered titanate nanosheets, and found that the lattice stability of the resulting nanohybrids could be greatly enhanced by hydrothermal treatment.

Pristine cesium titanate, $Cs_{0.67}Ti_{1.83}O_4$, was prepared by conventional solid-state reaction and its protonic phase was obtained by ion-exchange reaction between the cesium cation and protons. The exfoliation of layered titanate was achieved by reacting the protonic titanate with tetrabutylammonium hydroxide.[9] After the reaction, a small fraction of incompletely exfoliated particles were removed by high-speed centrifugation (12 000 rpm for 10 min). The sol solution of zinc acetate was prepared by reacting the aqueous solution of zinc acetate with *n*-propanol at 120 °C for 2 h. The ZnO–$Ti_{1.83}O_4$ nanohybrid was synthesized by reassembling the exfoliated colloidal titanate in the presence of the sol solution of zinc acetate at 80 °C for 2 h in a 50 mL autoclave with a Teflon liner. Alternatively, the nanohybrid was obtained by refluxing the mixture of the titanate colloidal suspension and the zinc acetate solution at 80 °C for 2 days. In both cases, flocculated precipitates were immediately formed upon the mixing of the two solutions. The resultant products were separated by centrifuging, washing thoroughly with distilled water, and drying. The crystal structures and physico-chemical properties of the ZnO–$Ti_{1.83}O_4$ nanohybrids were characterized by X-ray diffraction (XRD, Philips X'pert, λ = 1.5418 Å, 298 K), inductively coupled plasma (ICP), thermogravimetric-differential thermal analysis (TG-DTA), field emission-scanning electron microscopy (FE-SEM), and N_2 adsorption–desorption isotherm measurements. In addition, the chemical bonding nature and band structure of the nanohybrids were examined by performing Zn K-edge X-ray absorption near-edge structure (XANES) and diffuse reflectance ultraviolet-visible (UV-vis) spectroscopic analyses, respectively. The present XANES data were collected from the thin layer of powder samples deposited on transparent adhesive tapes in a transmission mode at the beam line 7C in the PLS (Pohang, Korea) operated at 2.5 GeV and 180 mA. The measurements were carried out at room temperature with a Si(111) single crystal monochromator. No focusing mirror was used. All the present spectra were carefully calibrated by measuring Zn foil simultaneously. The data analysis was done with the program WINXAS 2.3.

The powder XRD patterns of the protonic titanate and the ZnO–$Ti_{1.83}O_4$ nanohybrids prepared by reflux and hydrothermal reactions (denoted as ZnO–$Ti_{1.83}O_4$-**R** and ZnO–$Ti_{1.83}O_4$-**H**, respectively) are presented in Fig. 1 and compared with those of their calcined derivatives. Both the as-prepared ZnO–$Ti_{1.83}O_4$ nanohybrids exhibit a series of equally spaced (0l0) reflections at lower angles, which is quite different from the protonic titanate,[10] indicating the formation of heterostructure with an expanded interlayer space accommodating nanosized zinc species. From the least squares fitting analysis, the basal spacings were determined to be 20.4 Å for the ZnO–$Ti_{1.83}O_4$-**R** and 12.0 Å for the ZnO–$Ti_{1.83}O_4$-**H**, which correspond to the gallery heights of 12.9 and 4.5 Å, respectively. It is worthwhile to note here that the fine tuning of the reaction routes allows us to control the crystal structure of the nanohybrid, as illustrated in Fig. 2. The formation of layer-by-layer restacked heterostructure was further confirmed by FE-SEM images showing the regular stacks of layered titanate sheets, see the right panel of Fig. 1. The ICP results provide a strong evidence for the incorporation of zinc species into the

Center for Intelligent Nano-Bio Materials (CINBM), Division of Nano Sciences and Department of Chemistry, Ewha Womans University, DaeHyun-dong 11-1, Seoul, 120-750, Korea.
E-mail: hwangsju@ewha.ac.kr; Fax: +82-2-3277-3419; Tel: +82-2-3277-4370

† Electronic supplementary information (ESI) available: High angle XRD patterns, TG-DTA curve and N_2 adsorption–desorption isotherm of ZnO–$Ti_{1.83}O_4$ nanohybrid. See DOI: 10.1039/b511471c

 This journal is © The Royal Society of Chemistry 2006

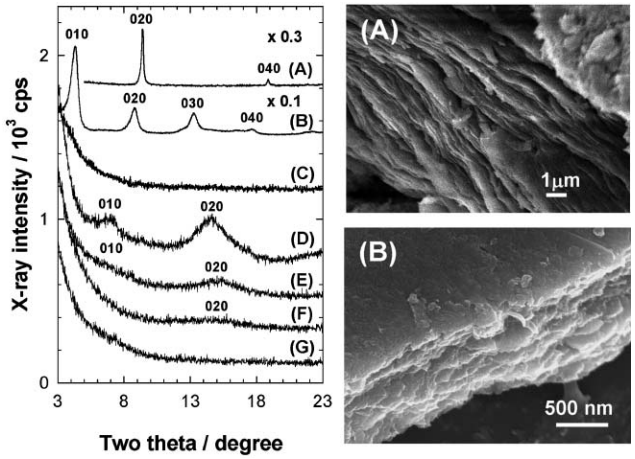

Fig. 1 Left panel: small angle XRD patterns of (A) the protonic titanate, (B) ZnO–$Ti_{1.83}O_4$-**R** and (C) its derivative calcined at 200 °C, (D) ZnO–$Ti_{1.83}O_4$-**H** and its derivatives calcined at (E) 200, (F) 300, and (G) 400 °C. Each pattern is shifted along the *y*-axis for clarity. Right panel: FE-SEM images of (A) ZnO–$Ti_{1.83}O_4$-**R** and (B) ZnO–$Ti_{1.83}O_4$-**H**.

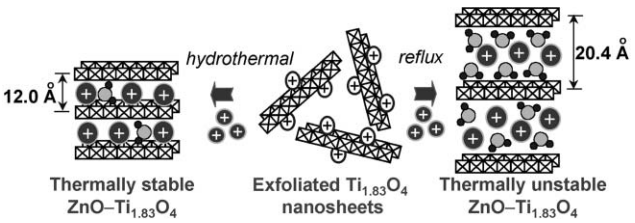

Fig. 2 Dependence of crystal structure and thermal stability of porous zinc oxide-layered titanate nanohybrids on the synthetic conditions.

layered titanate lattice with a Zn/Ti ratio of 2.1 for the ZnO–$Ti_{1.83}O_4$-**R** and 1.8 for the ZnO–$Ti_{1.83}O_4$-**H**, respectively. CHN elemental analysis demonstrates that the as-prepared samples contain small amounts of carbon,[11] indicating that most of the zinc acetates (about 80–90%) have decomposed into zinc oxide during the synthesis, but a post-calcination process is necessary for the complete removal of organic residuals. The thermal stability of the obtained nanohybrids was examined by monitoring the variation of XRD patterns upon calcination at 200–400 °C under Ar flow. After heat-treatment at 200 °C, the ZnO–$Ti_{1.83}O_4$-**R** shows complete disappearance of (0l0) reflections with the advent of distinct peaks corresponding to ZnO at the high angle region of 30–40° (see Electronic Supplementary Information†), clarifying the disintercalation of the guest species and the formation of ZnO on the sample surface. On the contrary, the calcined derivative at 200 °C of the ZnO–$Ti_{1.83}O_4$-**H** retains a series of (0l0) reflections without the appearance of ZnO peaks. The heat-treatment at 400 °C leads to the complete removal of the (0l0) peaks as well as to the development of weak ZnO peaks at high angle region. This finding provides strong evidence of the effectiveness of the hydrothermal method in improving the structural stability of the heterostructure. According to TG-DTA results,† the reflux-prepared sample contains larger amounts of interlayer water molecules ($2.3H_2O$ per unit formula) than the hydrothermally prepared one ($0.9H_2O$ per unit formula). Such different water contents of these compounds would be responsible for their dissimilar structural stability as well as for their different basal increment. Namely, the removal of a large amount of space-filling water molecules promotes the collapse of the heterostructure.

Also, we have probed the variation of surface area and porosity upon the hybridization and post-calcination by performing N_2 adsorption–desorption isotherm measurements.† The BDDT type I and IV shape of isotherms occur commonly for both the as-prepared ZnO–$Ti_{1.83}O_4$ nanohybrids and their calcined derivatives, along with H4-type hysteresis loop in the IUPAC classification.[12] Such a type of isotherm underlines the presence of the open slit-shaped capillaries with very wide bodies and narrow short necks. According to the fitting analysis based on the BET equation, the as-prepared ZnO–$Ti_{1.83}O_4$-**H** and its calcined derivatives possess expanded surface areas of 114 and 119–134 m^2g^{-1}, respectively, which are greater than those of the as-prepared ZnO–$Ti_{1.83}O_4$-**R** and its calcined derivative at 200 °C (40 and 71 m^2g^{-1}). All of the present nanohybrids exhibit commonly a weak adsorption of N_2 molecules in a low relative pressure (p/p_0) region and a distinct hysteresis in the region of $p/p_0 > 0.5$, demonstrating that most of the porosity in the present nanohybrids originates from mesopores in the stacked structure of nanohybrid crystallites. The negligible adsorption of nitrogen molecules into the micropores would be due to the presence of residual carbon species and water molecules blocking the micropores and/or due to the partial destruction of the heterostructure after the calcination. In addition, the gallery height of the calcined ZnO–$Ti_{1.83}O_4$-**H** (4.2 Å) is only slightly larger than the kinetic diameter of the nitrogen molecule (3.64 Å). Furthermore, the presence of interlayer zinc oxide would make the diameter of the micropores narrower, which prevents the efficient introduction and adsorption of nitrogen molecules into the gallery space of the nanohybrids.

However, it is worthy to note here that, in spite of the collapse of the heterostructure, the calcined derivative of ZnO–$Ti_{1.83}O_4$-**H** at 400 °C still shows a marked hysteresis and an expanded surface area with mesoporosity, underlining the high stability of pore-structure in the hydrothermally prepared nanohybrids. Therefore, these mesoporous materials are expected to be useful as efficient catalysts or absorbents.

Fig. 3 represents the diffuse reflectance UV-vis spectra of the ZnO–$Ti_{1.83}O_4$ nanohybrids and their calcined derivatives. The E_g values of the as-prepared nanohybrids (3.6–3.7 eV) are greater than that of the bulk ZnO (3.2 eV) due to the quantum confinement effect of hybridized ZnO species. Upon calcinating at 200 °C, no detectable change occurs in the UV-vis spectrum of ZnO–$Ti_{1.83}O_4$-**H**, whereas the calcined derivative of ZnO–$Ti_{1.83}O_4$-**R** shows appearance of a new absorption edge at ~3.3 eV, indicating the formation of zinc oxide on the sample surface. This result matches well with the poor thermal stablity of the latter, as revealed from XRD analysis. Also for ZnO–$Ti_{1.83}O_4$-**H**, a heat-treatment at higher temperature leads to an appearance of a lower energy absorption edge. However, the calcined derivatives still show the absorption edge at slightly higher energy than the bulk ZnO, clarifying the nanocrystalline nature of the guest zinc oxide.

The chemical bonding nature of the zinc species was probed with Zn K-edge XANES analysis, as shown in Fig. 4. The edge position of the present nanohybrids is similar to that of the reference ZnO, indicating the divalent oxidation state of zinc in these compounds. Both the as-prepared nanohybrids exhibit commonly poorly resolved XANES features in the energy region

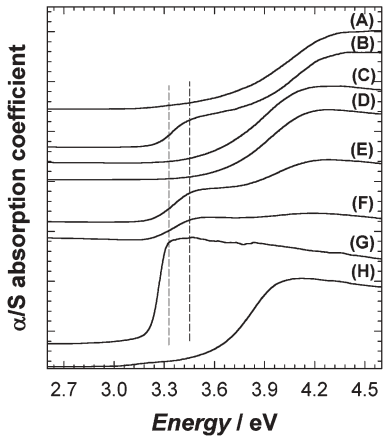

Fig. 3 Diffuse reflectance UV-vis spectra of (A) ZnO–$Ti_{1.83}O_4$-**R** and (B) its derivative calcined at 200 °C, (C) ZnO–$Ti_{1.83}O_4$-**H** and its derivatives calcined at (D) 200, (E) 300, and (F) 400 °C, together with the reference spectra of (G) ZnO and (H) $Cs_{0.67}Ti_{1.83}O_4$. Each spectrum is shifted along the *y*-axis for clarity. The dashed lines are guidelines for easier interpretation of the figure..

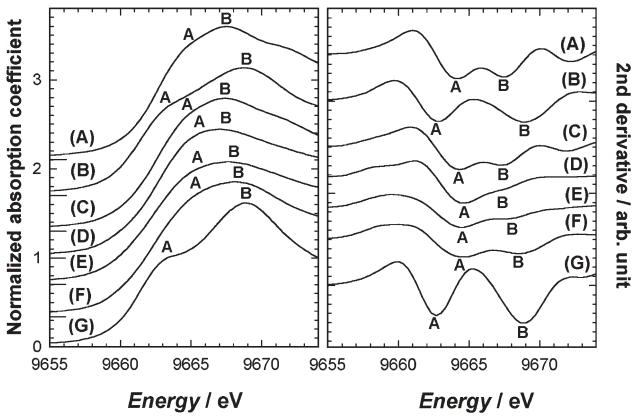

Fig. 4 Zn K-edge XANES spline (left) and second derivative (right) spectra of (A) ZnO–$Ti_{1.83}O_4$-**R** and (B) its derivative calcined at 200 °C, (C) ZnO–$Ti_{1.83}O_4$-**H** and its derivatives calcined at (D) 200, (E) 300, and (F) 400 °C, together with the reference spectrum of (G) ZnO. Each spectrum is shifted along the *y*-axis for clarity.

of 9664–9668 eV, which are quite different from the reference spectrum of the bulk ZnO. This is an indication that the the zinc species in the as-prepared nanohybrids are mostly in the form of a nanocrystalline zinc oxide in the interlayer space of titanate lattice.[13] After calcinating at 200 °C, the ZnO–$Ti_{1.83}O_4$-**R** shows two distinct peaks A and B at 9662.5 and 9669 eV, which is nearly identical to the spectral features of the bulk ZnO. This finding is in good agreement with an appearance of ZnO peaks in the corresponding XRD pattern. On the contrary, the poorly resolved XANES features of ZnO–$Ti_{1.83}O_4$-**H** remain nearly unchanged before and after the calcination, confirming the improved stability of the guest zinc oxide by hydrothermal synthesis.

In summary, we have been successful in synthesizing new 2D mesoporous ZnO–$Ti_{1.83}O_4$ nanohybrids through the exfoliation-restacking reaction, and in controlling the crystal structure and thermal stability of the nanohybrid by tuning synthetic conditions. This is the first example of the zinc oxide nanocrystals stabilized in the two dimensional lattice of semiconductive metal oxide. Currently we are carrying out the application of this mesoporous nanohybrid as photocatalysts and electrode materials for lithium secondary batteries, supercapacitors, solar cells, absorbents for chemicals and UV radiation, *etc*.

This work was performed by the financial support of National R&D programs' of the Ministry of Science and Technology (MOST), Republic of Korea and supported in part by the SRC/ERC program of the MOST/KOSEF (grant : R11-2005-008-03002-0). The experiments at Pohang Light Source (PLS) were supported in part by MOST and POSTECH.

Notes and references

1 M. H. Huang, S. Mao, H. Feick, H. Yan, Y. Wu, H. Kind, E. Weber, R. Russo and P. Yang, *Science*, 2001, **292**, 1897.
2 N. Saito, H. Haneda, T. Sekiguchi, N. Ohashi, I. Sakaguchi and K. Koumoto, *Adv. Mater.*, 2002, **14**, 418.
3 J. L. Yang, S. J. An, W. I. Park, G. C. Yi and W. Choi, *Adv. Mater.*, 2004, **16**, 1661.
4 K. Keis, E. Magnusson, H. Lindstrom, S. E. Lindquist and A. Hagfeldt, *Sol. Energy*, 2002, **73**, 51.
5 M. Zamfirescu, A. Kavokin, B. Gil, G. Malpuech and M. Kaliteevski, *Phys. Rev. B*, 2002, **65**, 161205.
6 J. H. Choy, E. S. Jang, J. H. Won, J. H. Chung, D. J. Jang and Y. W. Kim, *Adv. Mater.*, 2003, **22**, 1911; J. H. Choy, E. S. Jang and D. J. Jang, *Appl. Phys. Lett.*, 2004, **84**, 287.
7 B. S. Zou, V. V. Valkov and Z. L. Wang, *Chem. Mater.*, 1999, **11**, 3037; P. D. Cozzoli, M. L. Curri, A. Agostiano, G. Leo and M. Lomascolo, *J. Phys. Chem. B*, 2003, **107**, 4756.
8 L. Guo, Y. L. Ji, H. Xu, P. Simon and Z. Wu, *J. Am. Chem. Soc.*, 2002, **124**, 14864; M. Yin, I. L. Kuskovsky, T. Andelman, Y. Zhu, G. F. Neumark and S. O'Brien, *J. Am. Chem. Soc.*, 2004, **126**, 6206.
9 F. Kooli, T. Sasaki and M. Watanabe, *Chem. Commun.*, 1999, 211.
10 Since there are two titanate layers in the unit cell of the protonic titanate, its d_{020} value corresponds to the sum of gallery height and layer thickness, like the d_{010} value of the nanohybrids.
11 Contents (in wt%) of carbon and hydrogen for the as-prepared ZnO–titanate-**R** (C : 3.25%, H : 1.66%) and its calcined derivative at 200 °C (C : 3.47%, H : 1.23%), and the as-prepared ZnO–titanate-**H** (C : 3.70%, H : 1.44%) and its calcined derivatives at 200 °C (C : 2.54%, H : 0.97%), 300 °C (C : 2.07%, H : 0.78%), and 400 °C (C : 0.82%, H : 0.48%). Due to the decrease of total weight caused by the significant loss of water molecules, the heat-treatment at 200 °C leads to the slight increase of relative weight percent of carbon for ZnO–titanate-**R** with high water content. CO_2 gas evolved during the heat-treatment of the nanohybrids was clearly detected.
12 S. J. Gregg and K. S. W. Sing, in *Adsorption, Surface Area and Porosity*, Academic Press, London, 1982.
13 N. G. Park, M. G. Kang, K. M. Kim, K. S. Ryu, S. H. Chang, D. K. Kim, J. van de Langemaat, K. D. Benkstein and A. J. Frank, *Langmuir*, 2004, **20**, 4246.

 This journal is © The Royal Society of Chemistry 2006